ELSEVIER

Polymer 41 (2000) 2521–2534

polymer

A FTIR–ATR study of liquid diffusion processes in PET films: comparison of water with simple alcohols

C. Sammon[a,*], J. Yarwood[a], N. Everall[b]

[a]*Sheffield Hallam University, Materials Research Institute, City Campus, Howard Street, Sheffield S1 1WB, UK*
[b]*ICI, Analytical Sciences Division, P.O. Box 90, Wilton, Middlesbrough, Cleveland TS6 8JE, UK*

Received 1 January 1999; received in revised form 24 April 1999; accepted 25 May 1999

Abstract

An in-situ FTIR–ATR method for simultaneously obtaining both kinetic and structural information during liquid sorption into polymers was presented. The kinetics and diffusion profile of the sorption of liquid water and liquid methanol into poly(ethylene terephthalate) (PET) were compared and contrasted. The diffusion of water into PET was shown to follow Fickian kinetics, without significant swelling and the calculated diffusion coefficients (D) varied between 8.57 and 0.52×10^{-9} $cm^2\ s^{-1}$ for a crystallinity range of 4–25%. The D values decreased non-linearly with the increase in crystallinity. The average spherulitic crystal size was thought to play a significant role in determining the rate of water sorption. Conversely, the sorption of liquid methanol was accompanied by significant swelling and crystallisation and hence showed non-Fickian or anomalous kinetics. The sorption data were fitted to a dual sorption model which indicated that the rate of diffusion of liquid methanol was faster than that of liquid water, probably due to the accompanying swelling. Increasing the level of crystallinity was shown to decrease the capacity for the polymer to swell and reduced the calculated diffusion coefficients.

Keywords: FTIR–ATR depth profile; Fickian kinetics; Sorption

1. Introduction

The diffusion of small molecules through polymer membranes is an important phenomenon in many different areas of science and engineering. For example, the diffusivity in polymer films and membranes [1,2] is important in connection with the use of polymers as barrier coatings (for protection of an underlying substrate) in packaging applications [3] and for separation science applications [1,4]. Because of its widespread presence (both vapour and liquid) in the ambient environment in which polymers are used, water is probably the most important diffusant. In a passive sense, water is important as an essential part of hydrolytically induced degradation processes. In the active sense, the diffusion of water is clearly of critical importance for saline separation membranes [1,4], or for the protection of substrates and wrapped materials [5]. The diffusion of organic molecules in polymers has implications even further afield with such small molecules playing important roles in the polymer industry as plasticisers, fillers and biocides, etc. Further, organic solvents are also used to remove small organic impurities of oligomers from poly(ethylene terephthalate) (PET) films for use as high specification substrates [6]. The transport properties of small molecules in polymers [7–10] depend on a number of factors. These include:

1. the chemical structure in terms of details of the chemical repeat units (acid, amide, ester, etc.);
2. the polymer micro-organisation (molecular weight, morphology, crystallinty, glass transition temperature void distribution, etc.);
3. the chemical nature and levels of filler and other additives;
4. the temperature.

These factors control the solubility, the degree of swelling, the mode of mechanical relaxation, etc. and will combine to influence the rate at which the small molecule (for example water or an alcohol) is sorbed and transported under any given combination of chemical content and ambient conditions.

It is, of course, possible in principle [10,11] to use diffusion data of a small molecule in a polymeric matrix to distinguish different molecular microstructures using different models. It is expected, for example, that for polymers in their rubbery state (above T_g) the diffusion might be Fickian,

* Corresponding author.

0032-3861/00/$ - see front matter
PII: S0032-3861(99)00405-X

whereas for polymers in the glassy state, it is often shown that a good fit of the data to the Case II diffusion model [12,13] is achievable. Barbari et al. [10,11] have shown that it is possible to model the barrier layer of 'skin', which could lead to a delay time in the penetrant sorption. However, the situation is often considerably more complex. For example, Berends [14] has shown that the form of the sorption kinetics varies depending on the content of the particular penetrant. Thus, for example, for different organic solutes in PVC the kinetics are Fickian at low concentrations of penetrant, non-Fickian (maybe dual mode—see below) at intermediate penetrant concentrations and Case II when the concentration of penetrant is high. Further, at high sorption levels, an increase in film thickness produces a shift of the kinetics towards the Fickian model. This work illustrates that the details of sorption kinetics vary dramatically depending on the solute content and film thickness. For other polymers, for example for polyelectrolyte membranes important in saline separation applications, it has been shown [15,16] that the diffusion coefficients depend on a number of variables including the processing solvent, the level of chemical substitution and the film thickness. Clearly, polymer films show a diverse range of behaviour, which at present can only be described from an empirical point of view. Nevertheless, it is interesting to elucidate the model and rate of kinetics for the diffusion of small molecules in polymeric films such as PET, both from a practical point of view and from the point of view of the development of a fundamental database of polymer/penetrant behaviours from which the understanding of such processes can eventually be derived.

A considerable amount of work on the diffusion of liquid water and water vapour into PET has been published. Recent work includes the work of Langevin et al. [17], who obtained a diffusion coefficient at 20°C of 4.5×10^{-9} cm^2 s^{-1}, using a gravimetric technique (with a water content at equilibrium estimated to be about 1% by weight). Impedence spectroscopy has been used to calculate the diffusion coefficient and equilibrium water content of PET [18,19]. Diffusion coefficients calculated using this method varied from 2. to 9.97×10^{-9} cm^2 s^{-1} for liquid water at 40°C in good agreement with values obtained by the (traditional) gravimetric method. Some thickness dependence was noted. The water concentration at equilibrium was found to be 0.54 and 0.95% by weight for samples of 75 and 205 μm thickness, respectively. Rueda et al. [20,21] used transmission spectroscopy as a function of crystallinity to study the diffusion of water vapour into PET. The diffusion coefficient calculated at 25°C varied between 8.18 and 3.93×10^{-9} cm^2 s^{-1} over a crystallinity range between 0 and 29%. The relationship of diffusion coefficient with crystallinity showed a power law, with an exponent of 0.5. Distinct evidence was found during the water vapour diffusion experiment of pseudo monomeric water with symmetric and antisymmetric O–H stretching bands at 3630 and 3550 cm^{-1}. Again, the equilibrium contents of water ranged between 0.6 (at 29% crystalline material) and 1% (for amorphous material). The diffusion of water vapour into PET has also been measured at 25°C using the time lag technique [22]. For Mylar A, a value of $D = 3.95 \times 10^{-9}$ cm^2 s^{-1} was obtained. The use of in situ FTIR–ATR techniques to study the diffusion of liquid water in PET and PET coated with a thin (less than 100 nm) SiO_2 layer was explored by Schühler et al. [23]. For films varying in thickness between 12 and 25 μm, values between 1.59 and 2.18×10^{-9} cm^2 s^{-1} were obtained. These agree well with previously calculated values. Not surprisingly, the application of a SiO_2 layer drastically slowed down the diffusion process, which was then found to be non-Fickian.

The diffusion of methanol into PET and its effects on the polymer structure have been examined by a number of workers, [24–29]. The situation is rather different for organic solvents since, as indicated previously, sorption is often accompanied by swelling, an increase in the effective free volume and possible changes in the glass transition temperature and the degree of crystallisation. Indeed, Durning et al. [25,26] proposed a mathematical model for this change of crystallisation of PET on methanol absorption. The kinetics of liquid induced crystallisation were shown to be extremely rapid [24,27,28] and resulted in the polymer becoming opaque to visible light due to the creation of spherulitic structures, with sizes the same order as that of the wavelength of the light [27–30]. Relatively little work on the sorption of alcohols into PET has been published. However, Barson and Dong [31] have studied the diffusion of ethanol vapour into orientated PET membranes using the radio tracer technique, while Sifiakis and Rodgers [32] have studied the sorption of a series of alcohol vapours (methanol, ethanol, propanol, butanol and isopropronol) into amorphous PET. The rate of sorption was found to decrease with increasing size of the alcohol. It is clear from a previous work [6] that the diffusion of organic liquids into PET depends dramatically on the chemical microstructure. For example, for benzyl alcohol sorption the diffusion coefficient changed from 1×10^{-8} cm^2 s^{-1} for amorphous PET to 4×10^{-10} cm^2 s^{-1} for orientated PET. Further, the equilibrium weight gains were quoted at ~22 and ~13.5% for amorphous and orientated PET, respectively. This, of course, is much higher than the solubility of water in PET, probably because of large differences in the swelling process.

In this paper, we compare the different sorption processes (rates and mechanisms) that occur when water and methanol are sorbed in PET.

2. Experimental

The films used in this project were made by two different methods in order to encompass a broad crystallinity range. The films were made from extrusion grade, PET chips, containing pure PET (E47) and PET (E99) manufactured

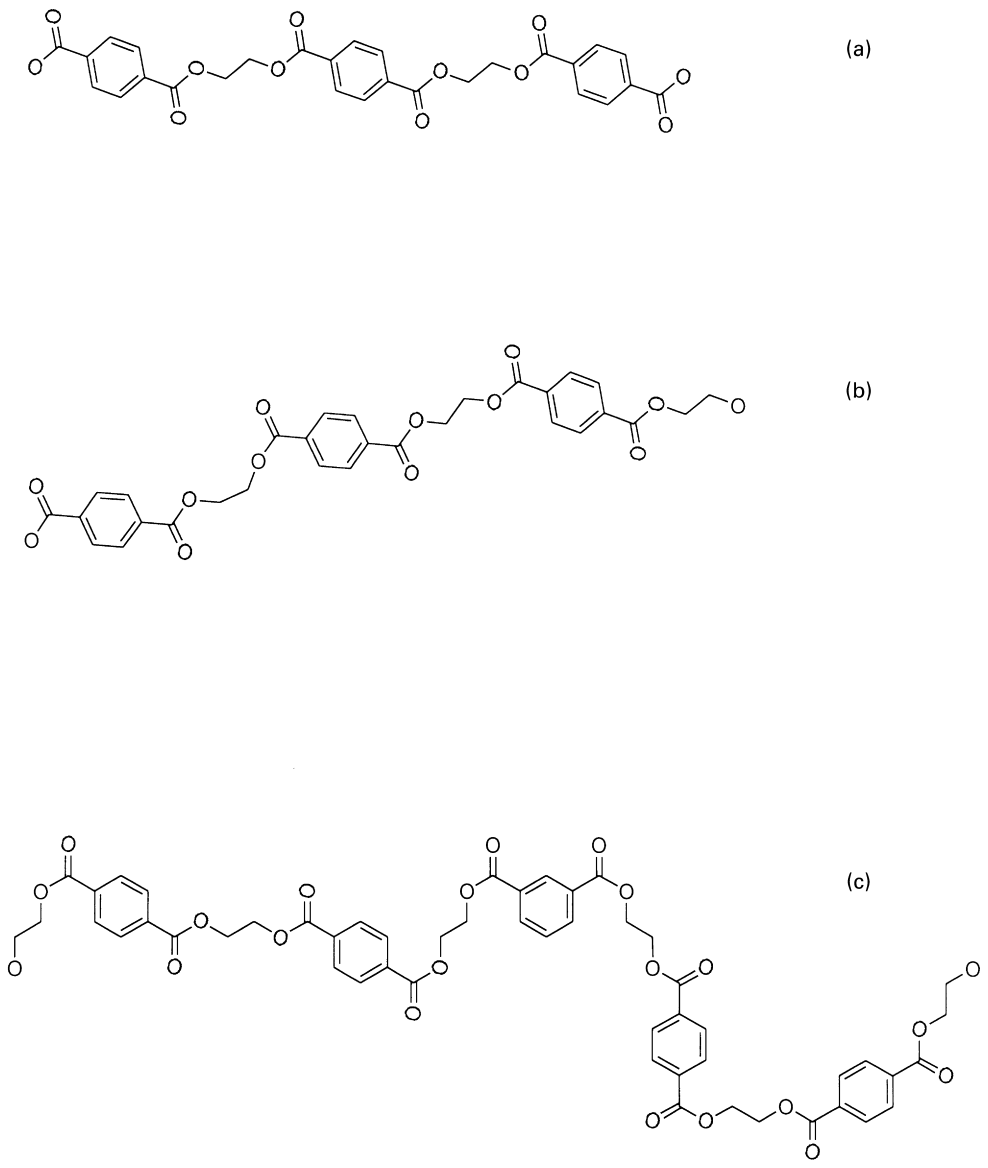

Fig. 1. (a) E47 PET in an all '*trans*' crystalline formation; (b) E47 PET in a mixed '*trans*' and '*gauche*' amorphous conformation; (c) E99 PET containing a fixed percentage of isophthalic acid comonomer.

from 18% isophthalic acid (random copolymer) (see Fig. 1). The molecular weights ($\overline{M}_w$) and T_g of these two materials (obtained from GPC and DSC measurements) were 70 and 60 (73 and 67°C, respectively. Films were manufactured by casting from ~5% (w/w) E99 polymer in tetrachloroethane (TCE). It was found that the manufacture of films of E47 from TCE produced a non-uniform film with a great deal of surface spherulitic growth. However homogeneous and

Table 1
Summary of the thicknesses and X_c of the films used for diffusion experiments annealed at 85–90°C

Film thickness (μm)	Pre anneal % X_c	Anneal time (h)	Post anneal % X_c
11.0 ± 0.2	4.0 ± 0.1	0	4.0 ± 0.1
8.7 ± 0.3	4.1 ± 0.1	0.25	6.4 ± 0.2
9.2 ± 0.2	5.0 ± 0.2	1	8.4 ± 0.2
8.0 ± 0.2	3.9 ± 0.3	3	10.1 ± 0.3
8.4 ± 0.1	4.2 ± 0.2	16	11.2 ± 0.2
8.2 ± 0.3	3.7 ± 0.1	6	12.7 ± 0.2
8.4 ± 0.1	3.6 ± 0.2	2	13.7 ± 0.3
8.6 ± 0.2	3.7 ± 0.2	8	16.2 ± 0.4

Table 2
Summary of the thicknesses and X_c of the films used for diffusion experiments (*trans*-esterified polymer)

Film thickness (μm)	E47:E99	X_c %
8.2 ± 0.1	0:1	4.9 ± 0.3
8.6 ± 0.3	1:3	8.4 ± 0.4
8.2 ± 0.2	1:2	11.2 ± 0.3
8.4 ± 0.2	1:1	18.2 ± 0.2
8.0 ± 0.2	1:0	25.0 ± 0.2

uniform films containing E47 PET were cast from *ortho*-chlorophenol (OCP) which seems to stop the formation of spherulites on the surface, allowing the casting of films of higher crystallinity. Film uniformity was checked using infrared transmission measurements over different regions of approximately 1 cm^2 with a variable aperture and by comparing resulting intensities. Uniformity was also checked taking a confocal Raman depth profile of the samples with approximately 2 μm^3 spatial resolution.

One method of varying the initial level of crystallinity within an E99 polymer film was to anneal the films above 73°C to induce crystallinity [33]. Unfortunately, using a zinc selenide substrate, it was impossible to anneal above 100°C, so it was only possible to obtain a range of crystallinities between 4 and 16% over the temperature range 85–90°C. Table 1 shows the thicknesses and % crystallinity calculated for the films used in this work. Raman depth profiling of these films showed no discernible differences in the morphology of the films on a 2 μm^3 scale.

In order to increase the range of crystallinity available in the films, the process of *trans*-esterification [34] was used. By mixing E47 PET and E99 PET in solution at high temperature, it was possible, by varying the ratio of the two polymers to manufacture a wide range of crystallinities from OCP (which also has the advantage of a high boiling point). Heating in excess of 12 h tends to produce uniform films for solutions of approximately 5% (w/w) PET/OCP near the boiling point of OCP (175°C) followed by film annealing at 60°C for more than 24 h to remove any excess solvent. Film quality was enhanced even further by casting while still hot onto a zinc selenide crystal held at ambient temperature. These films were characterised in the same way as the annealed films with crystallinities and thicknesses calculated using the standard procedures (see below). The films manufactured are summarised in Table 2.

Thickness calibration was performed using a surface profiler (Laser Form Talysurf), which measures the height as a function of distance along a predefined raster. A typical surface profile output is shown in Fig. 2. Thicknesses were calculated by taking the mean value of the measured step height relative to the baseline. Since ATR diffusion measurements cannot be made with films, which have been measured using the surface profiler, it was necessary to make thickness measurements by calibration of an absorbance versus thickness plot using transmission infrared measurements. The PET band at 1410 cm^{-1} was used to perform this calibration [35], since it is neither conformationally sensitive nor dichroic in nature, and has a small enough extinction coefficient not to saturate over the given thickness range. The necessary calibration plot used in this work is shown in Fig. 3.

The crystallinity of the films prepared in this way was calculated using the method of Belali and Vigoureux [36]. This involves monitoring quantitatively changes in the CH_2 wagging region of the PET infrared

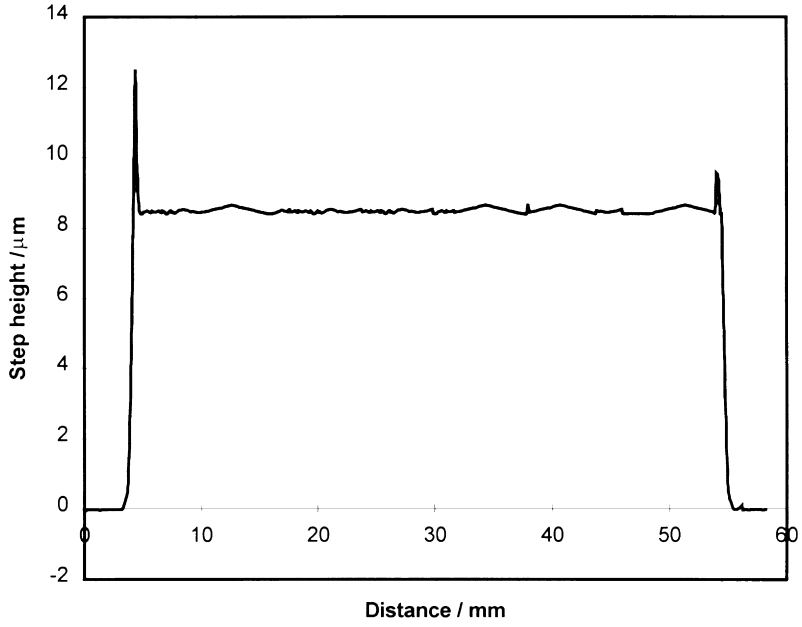

Fig. 2. Typical Talysurf output used to underpin the thickness calibration.

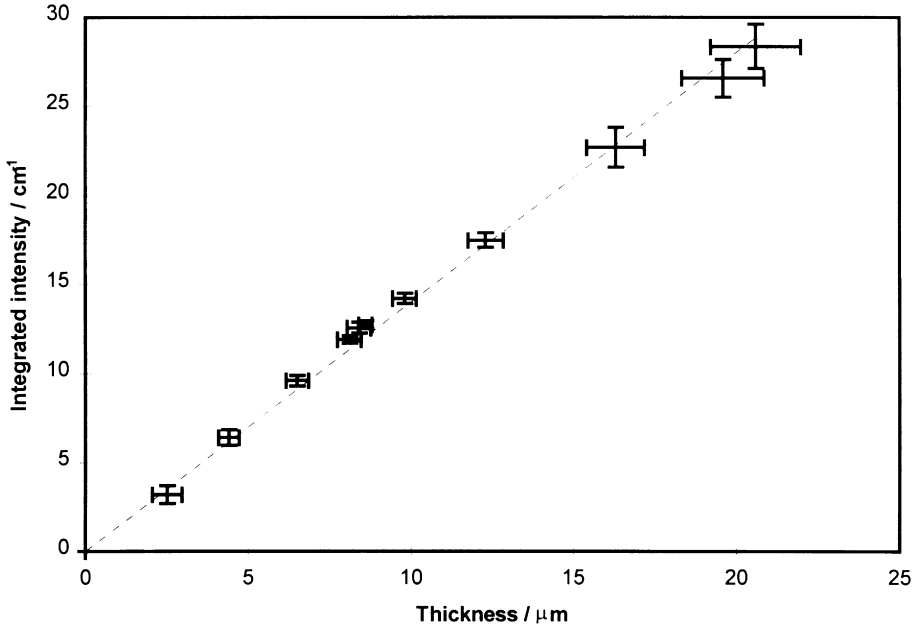

Fig. 3. FTIR-transmission calibration plot for film thickness measurements using the 1410 cm^{-1} band of PET.

spectrum in the region between 1300 and 1400 cm^{-1} (see Fig. 4). The model suggested for the calculation of crystallinity in PET uses the amorphous and crystallinity bands associated with *trans* and *gauche* conformers of the CH_2 wagging modes. The assumption is that at each point in the spectrum, the absorbance can be treated as that of the crystalline and amorphous parts superimposed. For ATR measurements the % crystallinity obtained from spectra such as that shown in Fig. 4, is given by Eq. (1).

$$\chi_c = \frac{a_i - a_j(A_i/A_j)(\nu_i/\nu_j)}{(c_j - a_j)(A_i/A_j)(\nu_i/\nu_j) - (c_i - a_i)} \quad (1)$$

a and c refer to molar absorption coefficients of the amorphous and crystalline parts at frequencies ν_i and ν_j and where A is the absorbance measured at frequencies ν_i and ν_j. Coefficients a and c need to be calculated by calibration with samples of known crystallinity. The data used in this work to calculate a and c were those of Zajicek [37].

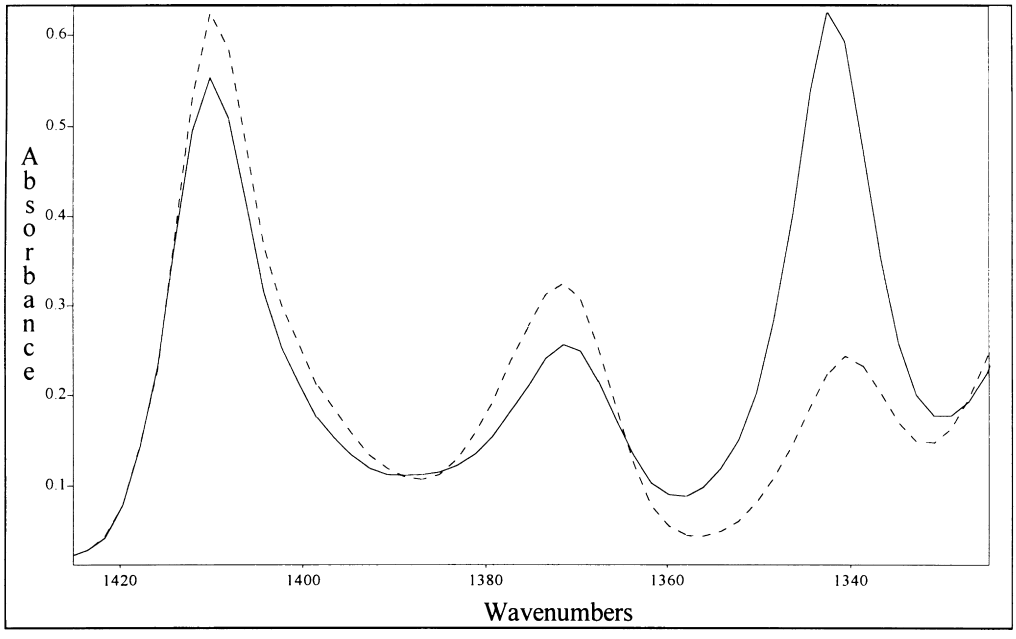

Fig. 4. Changes in the CH_2 wagging mode region of the ATR spectrum of PET as a function of crystallinity (dotted line is amorphous, solid line is 25% crystalline).

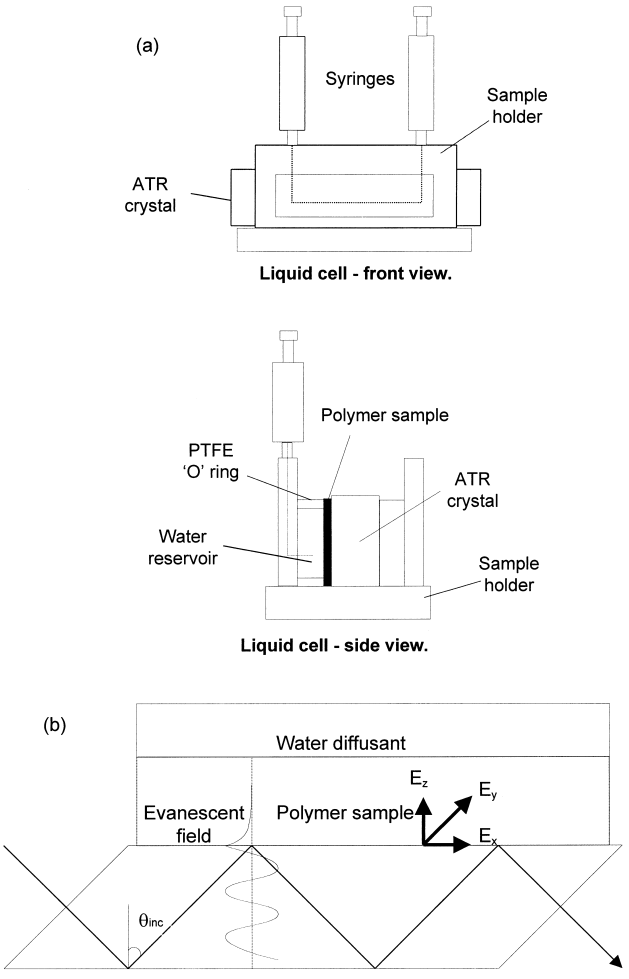

Fig. 5. (a) experimental FTIR–ATR cell used for diffusion measurements; (b) schematic of the ATR diffusion experiment.

Diffusion data were obtained using the FTIR–ATR method as described previously [10,11,16,38–40]. The experimental cell used is shown in Fig. 5. In practice, the sample was cast onto one side of the ATR prism (ZnSe) and mounted into the liquid cell. PTFE 'O' rings were used to seal the cell which was then filled using syringes shown. Spectra were recorded as a function of time on an Mattson FTIR spectrometer at a resolution of 4 cm^{-1} (every minute for the first 30 min of the experiment and every 5 min for the next 5 h). At each time point, 25 sample scans were collected over a period of 42 s, so that the absorbance at a particular time was an average over this time period. Spectra were ratioed against a background acquired with the dry film in place.

2.1. Analysis of the diffusion of water and methanol into PET

The raw data used to determine diffusion coefficients for the two liquids into semi-crystalline PET are shown as absorbance spectra in Fig. 6. The integrated areas of these bands as a function of time were used in order to deduce either the Fickian or anomalous (dual mode) diffusion coefficients for water and methanol, respectively. The ATR method of determination of sorption diffusivity into polymer films is now well established [10,11,16,38–40] and will only be summarised here for convenience.

For a plane sheet thickness L, of a polymer film with uniform distribution and equal concentrations on both sides, the mass transported liquid at time t, compared with the equilibrium mass is given [9,12] by Eq. (2)

$$\frac{M_t}{M_\infty} = 1 - \sum_{n=0}^{\infty} \frac{8}{(2n+1)^2\pi^2} \exp\left[\frac{-D(2n+1)^2\pi^2 t}{4L^2}\right] \quad (2)$$

where M_t is the mass sorbed at time t and M_∞ is the equilibrium mass.

At short times when M_t/M_∞ is small,

$$\frac{M_t}{M_\infty} = \frac{4}{L}\left(\frac{Dt}{\pi}\right)^n \quad (3)$$

In the ATR experiment, total reflection of a light beam occurs at the interface between a medium with high refractive index (ATR crystal, n_2) and one with a lower refractive index (polymer sample, n_1). The penetration of the electromagnetic field causes the formation of an evanescent wave propagating in all directions, decaying exponentially with distance from the surface. The evanescent wave electric field decay can be represented in the following form:

$$E = E_o \exp(-\gamma z) \quad (4)$$

where E_o is the electrical field strength at the surface (see Fig. 5),and

$$\gamma = \frac{2n_2\pi\sqrt{\sin^2\theta - \left(\frac{n_1}{n_2}\right)^2}}{\lambda} \quad (5)$$

where θ is the angle of incidence of the infrared radiation.

For the ATR diffusion experiment, Eq. (2) is modified [10] to take account of the convolution of the evanescent wave electric field (Eq. 4) with the diffusion profile. The resulting absorption is then

$$\frac{A_t}{A_\infty} = 1 - \frac{8\gamma}{\pi[1-\exp(2L\gamma)]} \sum_{n=0}^{\infty} \left[\frac{\exp\left(\frac{-D(2n+1)^2\pi^2 t}{4L^2}\right)\left[\frac{(2n+1)\pi}{2L}\exp(-\gamma 2L) + (-1)^n(2\gamma)\right]}{(2n+1)\left(4\gamma^2 + \left(\frac{(2n+1)\pi}{2L}\right)^2\right)} \right] \quad (6)$$

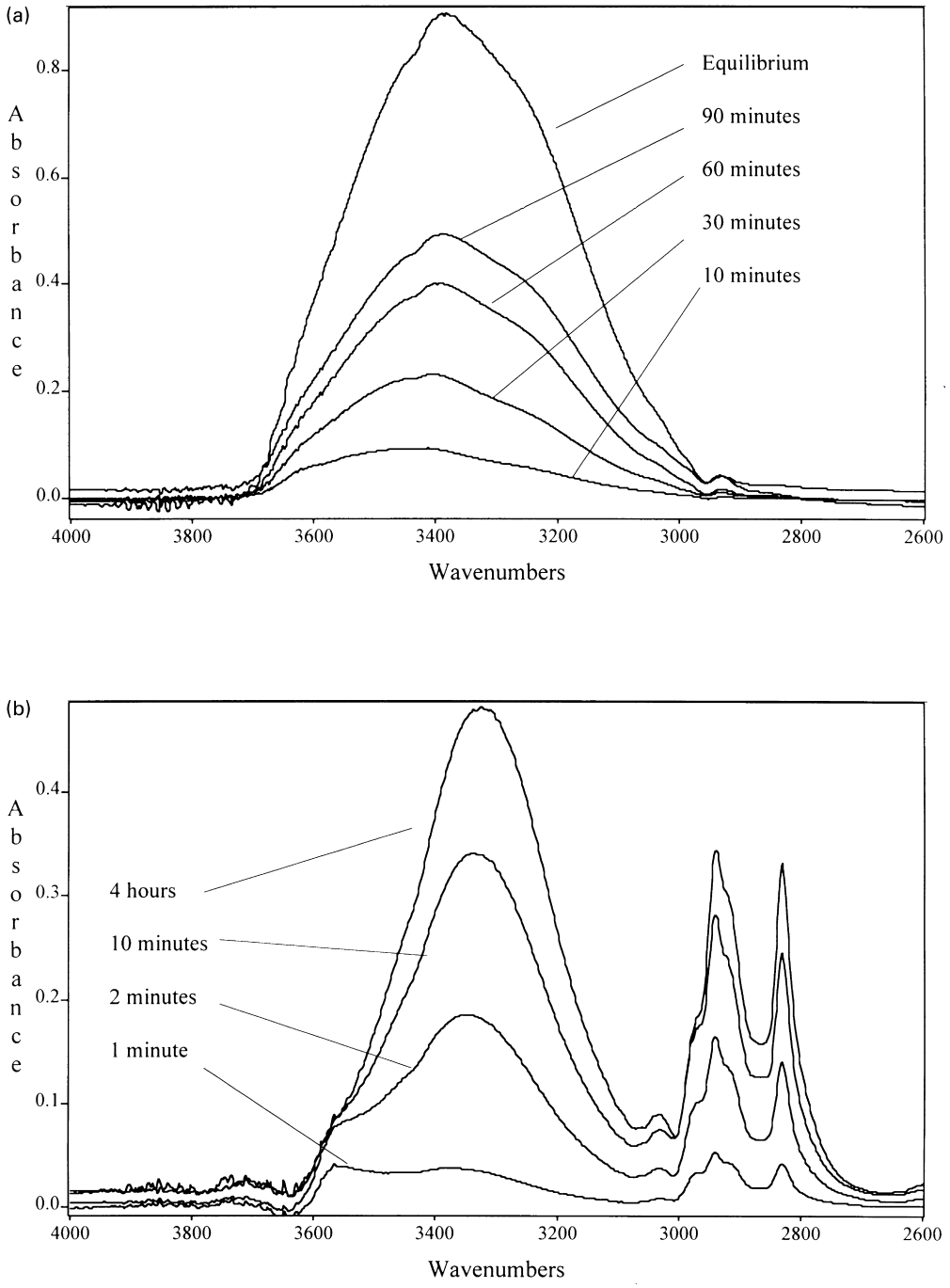

Fig. 6. (a) change of intensity of water band in PET at 10, 30, 60, 90 min and equilibrium (3 days); (b) change of intensity of methanol band in PET at 1, 2, 10 min and equilibrium (4 h).

where A_t is the absorbance at time t and A_∞ is the equilibrium mass.

In Fickian or Case I diffusion, n is $= 0.5$ (Eq. (3)). Such behaviour is usually found for rubbery polymers (amorphous, low T_g) where the rate of mechanical relaxation τ_m^{-1} is rapid compared with the rate of diffusion. For glassy polymers (crystalline, high T_g) when τ_m^{-1} is slow compared with the diffusion rate, n is usually greater that 0.5. The limiting case is referred to as Case II diffusion [12,13] and $n = 1$, but n can take intermediate values when the diffusion process is referred to as being anomalous or non-Fickian. This is because the T_g can be altered by ingress of the penetrant (see earlier section). It is not uncommon to find a change of a relevant model during the diffusion process. For the diffusion of water into PET in this work, it was discovered that the use of Eq. (5) for the diffusion curve, gave, in most cases, very good agreement with a model based on $n = 0.5$. In other words, the ATR

absorbance data fitted a Fickian concentration profile. For methanol (see results and discussion section), it was found that there is distinct deviation from the Fickian behaviour and we have used the dual mode approach, in which it is assumed that the polymer sorption occurs in two stages.

1. A rapid absorption into the surface sites (partially mobile species).
2. Subsequent diffusion into the bulk materials (totally mobile species).

Eq. (6) can then be recast to give,

$$\frac{A_1 - x_1 A_0}{x_1(A_\infty - A_0)} = 1 - \frac{8\gamma}{\pi[1 - \exp(2L\gamma)]} \sum_{n=0}^{\infty} \left[\frac{\exp\left(\frac{-D_1(2n+1)^2\pi^2 t}{4L^2} \right) \left[\frac{(2n+1)\pi}{2L} \exp(-\gamma 2L) + (-1)^n (2\gamma) \right]}{(2n+1)\left(4\gamma^2 + \left(\frac{(2n+1)\pi}{2L} \right)^2 \right)} \right] \tag{7}$$

for the first sorption mode, and

$$\frac{A_2 - x_2 A_0}{x_2(A_\infty - A_0)} = 1 - \frac{8\gamma}{\pi[1 - \exp(2L\gamma)]} \sum_{n=0}^{\infty} \left[\frac{\exp\left(\frac{-D_2(2n+1)^2\pi^2 t}{4L^2} \right) \left[\frac{(2n+1)\pi}{2L} \exp(-\gamma 2L) + (-1)^n (2\gamma) \right]}{(2n+1)\left(4\gamma^2 + \left(\frac{(2n+1)\pi}{2L} \right)^2 \right)} \right] \tag{8}$$

for the second sorption mode.

The values of x_1 and x_2 are related to the proportion of the partially and totally mobile molecules ($x_1 + x_2 = 1$). The value of x_1 and two separate diffusion coefficients ($D_1 + D_2$) can then be derived from the absorbance data.

Since, for ATR measurements, the initial part of the diffusion curve (see Fig. 7) is not a linear function of $t^{1/2}$ the ATR data measured in this work have been fitted, either to Eq. (6) or to Eqs. (7) and (8) (rather than using Eq. (3)).

3. Results and discussion

3.1. Diffusion of water into PET

The diffusion curves obtained using the methods described in the introduction are shown in Fig. 7, where it is clear that there is a distinct variation in diffusion coefficient as a function of crystallinity. Fig. 8 shows the change of diffusion coefficient as a function of crystallinity using data both from the annealed samples and from the *trans*-esterified samples. The necessary data are tabulated in Table 3.

If only data obtained from annealed samples are considered (Fig. 8) then it would appear that the variation of diffusion coefficient with % crystallinity is linear. However, if the data obtained from *trans*-esterified samples (crystallised from OCP) are included the overall variation is distinctly non-linear. The D values for higher crystallinities are found to be higher than that which might be expected for the linear model used for the annealed samples. Since it is thought [41] that the diffusion of water in semi-crystalline polymers occurs only in the amorphous regions of the film, this could be interpreted as resulting from diffusion in crystalline regions also. If this were the case then the diffusion profiles should not so obviously fit a pure Fickian model, since in the crystalline regions, the polymer is expected to be glassy. A more likely explanation is that the relation between the diffusion coefficient and crystallinity is simply not linear. If one considers that the spectra (and therefore the diffusion coefficient) will be modified by both water–polymer and water–water interactions that vary during the diffusion experiment, then it is possibly naive to expect a linear relationship. Further, it is possible to believe that the two different solvent systems used for the experiments (TCE and OCP) may give rise to two different sets of crystallite sizes. Certainly, the introduction of a comonomer into the PET lattice will effectively introduce more point defects and therefore limit the size and lamellar thickness of the crystalline material (Fig. 1). Thus, variations of comonomer level will produce crystallites of different sizes. It is possible to have two films with the same overall level of crystallinity with different crystallite sizes, which might have an effect of the rate of diffusion, even though diffusion may only occur in the amorphous region. Thus, the detailed morphology of the polymeric organisation is likely to have an influence on the rate of diffusion and may well be non-linear in its variation.

It may be observed from Fig. 7, that the quality of fit of the diffusion data for water in PET varies depending on the level of crystallinity. The output from an ATR diffusion experiment is a convolution of the evanescent wave and the liquid diffusion profile [10], resulting in a distinguishing 'S' shape of the data at low intensity and shorter times. For the amorphous films, the fit to such a model is poorer at short times, compared with that at longer times. A better fit at these short times is obtained using a slower diffusion coefficient. This is clearly shown in Fig. 7(a) and (d). The short time 'tail' is caused by the time it takes for water to enter the evanescent field. Comparison with simulated diffusion profiles has suggested [45] that these tails are associated with slower diffusion rates. It appears that the best fit to a Fickian model gives a diffusion constant higher

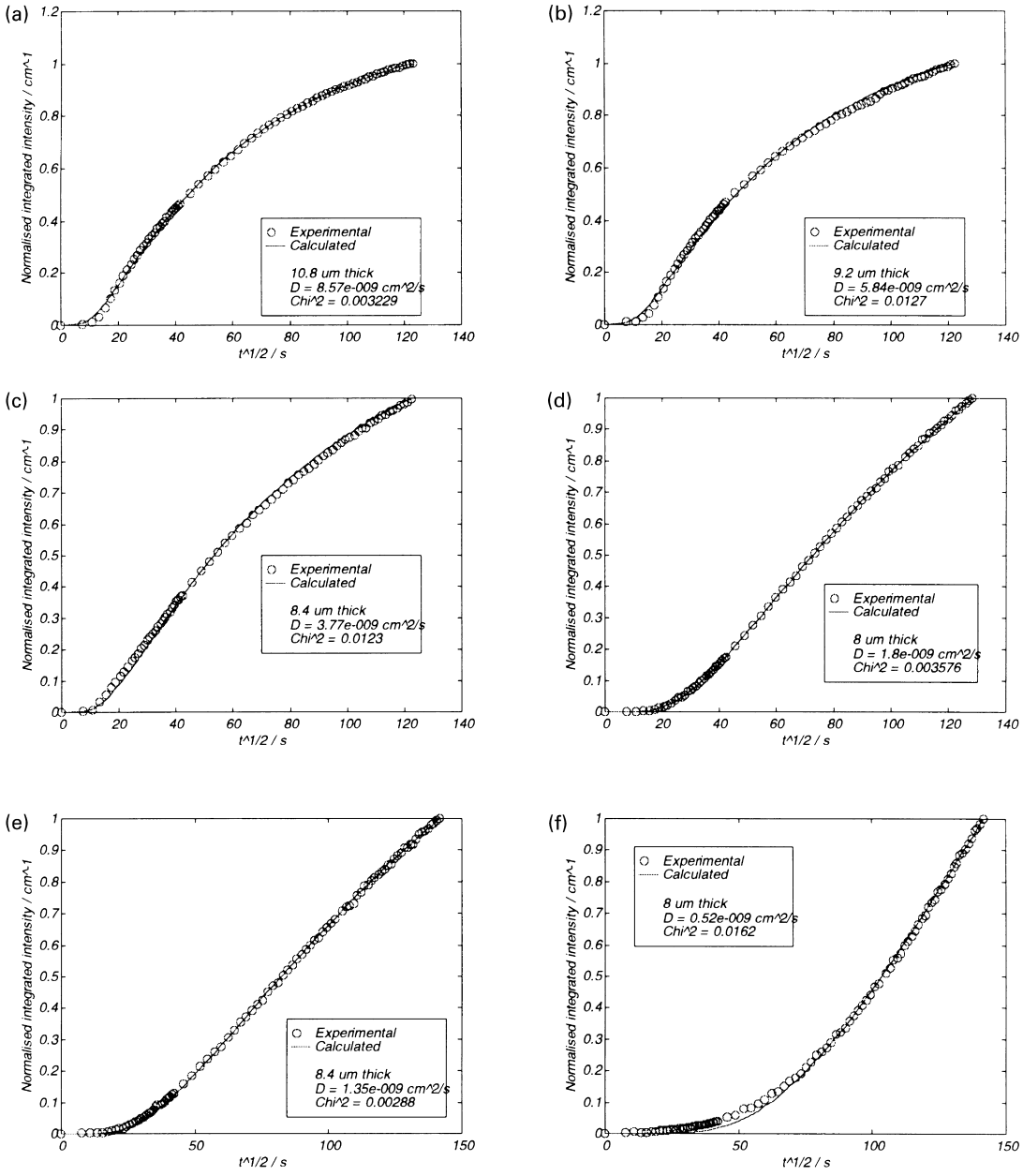

Fig. 7. Diffusion curves as a function of crystallinity for water/PET system (data fitted to Eq. (8)): (a) 4.0% crystalline; (b) 8.4% crystalline; (c) % crystalline; (d) % crystalline; (e) % crystalline; (f) % crystalline.

than that expected at shorter times. A possible explanation for such an observation is an increase in crystallinity at the surface, as demonstrated by Hayes et al. [42] using XPS. This excess crystallinity at the surface is reduced as the overall crystallinity increases and the bulk crystallinity approaches that of the surface. This results in the considerably better fit to a Fickian model without the postulated induction period caused by the so called 'skin effect'. Although several workers including Walls et al. [35,43] and Hayes et al. [42] have noted differences in the bulk and surface crystallinity in PET, it is interesting to note that we have not been able to discern any difference between bulk and surface crystallinity using a Raman microprobe with a depth resolution of approximately 2 μm. This suggests that if any differences in morphology are present between the surface and bulk material, the so called skin must be relevant to the top 0.5 μm of the films. Of course, it is also possible that the slower initial diffusion rate, which gets faster and more Fickian as the experiment progresses is due to the effect of plasticisation by water on the polymer chains in the amorphous region leading to a higher diffusion rate. However, this would be contrary to the work of van Alsten and Coburn [44] who have postulated that an increase in the amount of water in the bulk polymer may *restrict* motions of the polymer chain and reduce the effective D value. We have not detected this effect in our work.

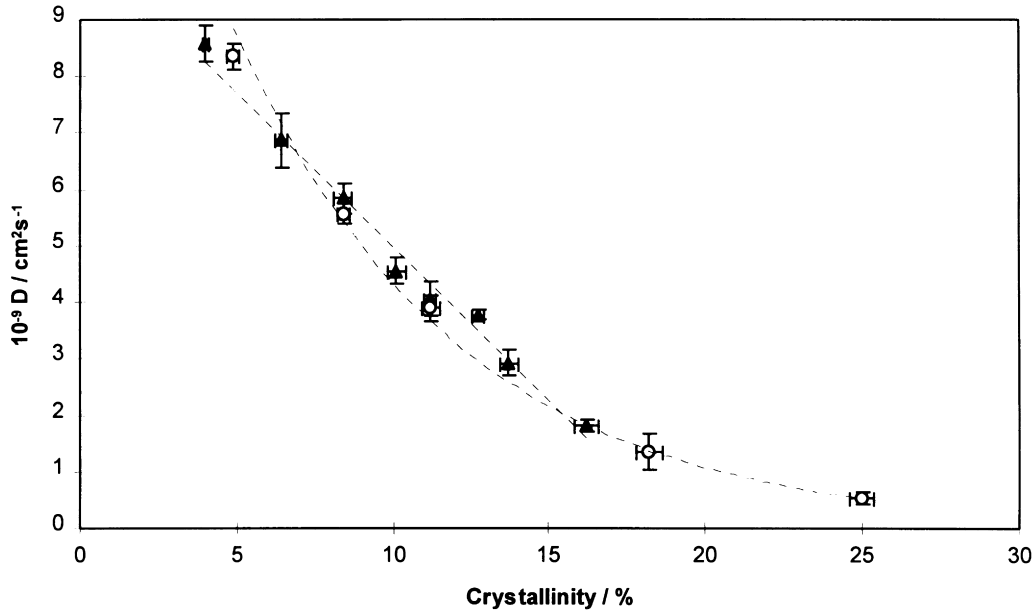

Fig. 8. Variation of diffusion coefficient as a function of crystallinity for water into PET. Filled triangles representing the annealed data and open circles representing the *trans*-esterified data.

3.2. Diffusion of methanol in PET

The diffusion of organic liquids into polymers is generally found to be non-Fickian [55], for several reasons. The most important of these is that such penetration is accompanied by significant swelling, which can change the diffusion coefficient by increasing the free volume within the polymer matrix [9]. Further, the absorption of small molecules into a polymer can lower the T_g of semicrystalline polymers, even to points below ambient temperature [25,26,46]. The degree and direction of induced crystallinity depend on the conditions used [46–50]. The raw data for the diffusion of methanol into PET under conditions used in this work are shown in Fig. 6(a). At short times (relatively low concentration) in 5% crystalline PET, the methanol ν(OH) vibrational band shows a distinct shoulder just below 3600 cm^{-1}. This could be due to a small population of non-hydrogen-bonded material in the polymer matrix. This effect, does not seem to occur for liquid water, since the overall hydrogen bonding network of clusters in water is expected to be more extensive at the same overall concentration level. On the contrary, this band could also be associated with methanol hydrogen bonding to the polymer. This would result in the weakening of methanol hydrogen bonding and a high frequency shift of the ν(OH) band. As the concentration of methanol in the polymer increases, this high wavenumber feature becomes less pronounced as found by Barbari et al. [10]. The data shown in Fig. 6(b) were fitted to a dual mode adsorption model (Eqs. (7) and (8)) (as was done in the past [51–53]) and a typical result is shown in Fig. 9. The diffusion constants are tabulated in Table 4 for two different crystallinity levels. A clear demonstration of the way in which the polymer swelled on methanol adsorption, is obtained by measuring the rate at which the $\nu(C=O)$ band of the PET decreased as a function of time (see Fig. 10). The larger the negative absorbance of the bands, the greater the swelling. Incidentally, this band is a doublet with components at approximately 1700 and 1740 cm^{-1}, as discovered previously [54]. The shift from approximately 1730 cm^{-1} for amorphous PET down to about 1700 cm^{-1} on methanol sorption is a reflection both of a change of crystallinity [25,26,29,46–49] and also the interactions of methanol with the carbonyl oxygen. A plot of the integrated intensity of the bands shown in Fig. 11(a) indicates that the swelling process occurs on approximately the same time scale as that associated with the diffusion of methanol in PET. Indeed the

Table 3
Tabulated thicknesses, % crystallinity and diffusion coefficients for water in PET

Film thickness (μm)	X_c%	D ($\times 10^{-9}$ cm^2 s^{-1})
Annealed samples		
11.0 ± 0.2	4.0 ± 0.1	8.57 ± 0.33
8.7 ± 0.3	6.4 ± 0.2	6.87 ± 0.48
9.2 ± 0.2	8.4 ± 0.2	5.84 ± 0.26
8.0 ± 0.2	10.1 ± 0.3	4.54 ± 0.23
8.4 ± 0.1	11.2 ± 0.2	4.05 ± 0.30
8.2 ± 0.3	12.7 ± 0.2	3.77 ± 0.10
8.4 ± 0.1	13.7 ± 0.3	2.92 ± 0.22
8.6 ± 0.2	16.2 ± 0.4	1.80 ± 0.11
Trans-esterified samples		
8.2 ± 0.1	4.9 ± 0.3	8.35 ± 0.11
8.6 ± 0.3	8.4 ± 0.4	5.58 ± 0.31
8.2 ± 0.2	11.2 ± 0.3	3.88 ± 0.24
8.4 ± 0.2	18.2 ± 0.2	1.35 ± 0.21
8.0 ± 0.2	25.0 ± 0.2	0.52 ± 0.24

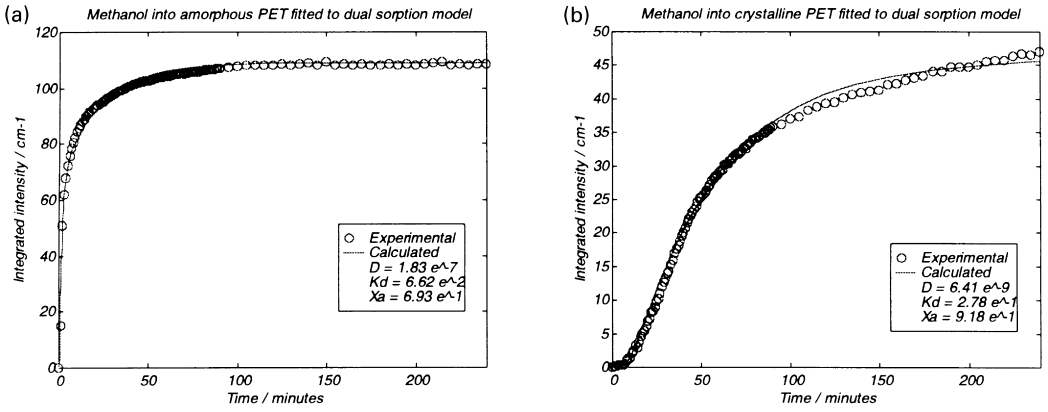

Fig. 9. Typical fits to the dual sorption model (Eqs. 7 and 8) for methanol diffusion into PET for: (a) 5.0% crystallinity; (b) 27.0% crystallinity.

rates of the two processes are directly related. Unfortunately, a measure of the rate at which the crystallinity of PET changes (Fig. 4) on methanol adsorption [36] was not possible using the infrared data because of interference from bands associated with methanol. Comparison of the rate of change of the carbonyl band with time, as a function of crystallinity is shown in Fig. 11. From these data, it is clear that the swelling process was faster in the more amorphous polymer since no initial positive bands were observed for the 5% crystalline film. For the 27% crystalline film, the diffusion of methanol was much slower (see Table 4) and the behaviour of the carbonyl band was somewhat different, since now the proportion of material, which can swell was considerably less.

The quality of fit of the data for methanol sorption depends on the level of crystallinity (compare Fig. 9(a) and (b)). There is thus a significant difference in the way in which sorption occurred for largely amorphous and partially crystalline PET. This is reflected also by the diffusion coefficients shown in Table 4. In the dual sorption model, the diffusion coefficients D_1 and D_2 represent two mobile species of penetrant. One represents the rate at which the penetrant is initially sorbed onto the polymer and the other one represents the rate at which the penetrant subsequently diffuses into the polymer matrix. Unfortunately, it is not possible (by using Eqs. (7) and (8) to fit to a particular set of data) to discriminate between the two physical processes. Nevertheless, it is clear from Table 4 that one of the diffusion coefficients, termed D_2 here, is much slower than the other one termed D_1 here. Further, on going from 5% crystalline, to 27% crystalline material, both diffusion coefficients were dramatically reduced by between one and two orders of magnitude. This is consistent with the fact that the more crystalline the material, the swelling is considerably less and thus the creation of free volume was considerably less. It is therefore expected that the penetration of molecules within the polymer matrix [56] will be much faster for the material with the larger degree of swelling and the lower degree of crystallinity. It is also interesting to note that for a given crystallinity level, the diffusion of methanol in PET is considerably faster than that of water (compare Tables 3 and 4). This could be associated, again with the degree of swelling of the material as a function of time during the diffusion process or differences in the induced crystallinity of the material by water and methanol, respectively. Such behaviour may also be associated with the degree of clustering of the two different penetrants [57] and the ability of a polymer matrix to reduce the cluster size. It is interesting that the band shape of the methanol ν(OH) band was considerably less sensitive that that of the water ν(OH) vibrational band as a function of time. This strongly implies that the water clusters break up over a much longer time period than that observed for the disruption of methanol hydrogen bonding.

Table 4
Calculated diffusion coefficients and fraction of 'bound' penetrant for methanol diffusing into PET

Sample	5% crystalline	27% crystalline
D_1 ($\times 10^{-8}$ cm^2 s^{-1})	18.3($\pm$0.22)	0.64($\pm$0.09)
D_2 ($\times 10^{-8}$ cm^2 s^{-1})	1.21($\pm$0.09)	0.18($\pm$0.07)
X_a	0.69($\pm$0.03)	0.92($\pm$004)

4. Summary and conclusions

An FTIR–ATR method has been successfully applied to the in-situ analysis of the sorption of water and methanol into PET of varying degrees of crystallinity. The two systems were shown to have very different sorption kinetics. The diffusion of liquid water into PET was shown to follow Fickian kinetics with a decrease in the diffusion coefficient with increasing crystallinity. No significant evidence of swelling was noted. The diffusion coefficients (calculated by fitting data to a model (Eq. 5) and obtaining the best fit) were found to range from 8.57×10^{-9} cm2 s^{-1} to 0.52×10^{-9} cm2 s^{-1} for a crystallinity range of 4–25%. There is evidence that the relationship between diffusion coefficient and crystallinity is non-linear and it is implied that the size

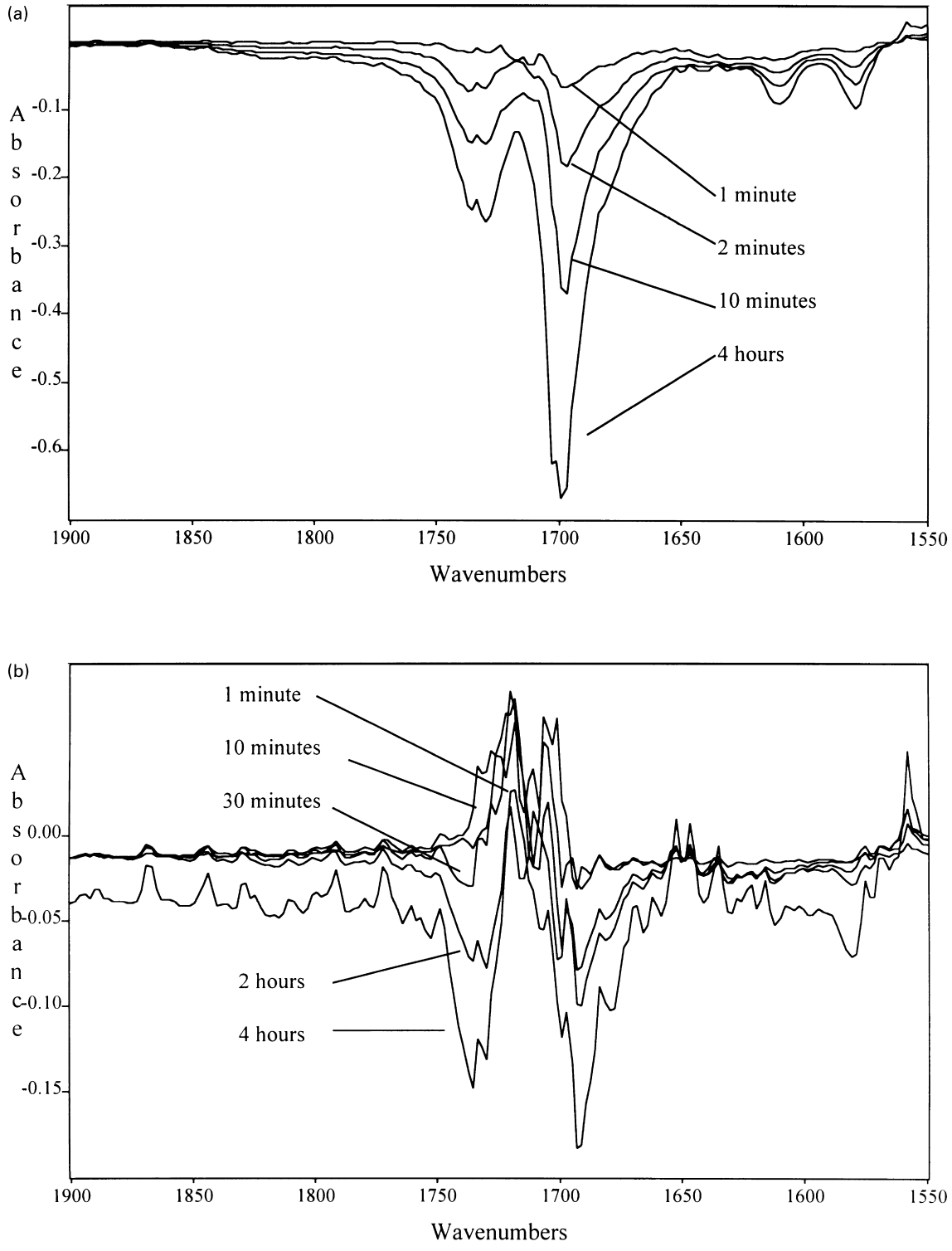

Fig. 10. Demonstration of the swelling of the PET polymer film on sorption of methanol for: (a) 5.0% crystallinity; (b) 27.0% crystallinity.

of the spherulitic crystals within the polymer matrix play an important role in the rate of diffusion.

The sorption of liquid methanol into PET follows non-Fickian or anomalous kinetics. The data have been fitted to a dual sorption model, which gives two diffusion coefficients based on two species with differing mobility. Sorption of methanol is accompanied by swelling, the rate of which is directly related to the diffusion rate. Increasing the degree of crystallinity, decreases the level of swelling, hence the diffusion rate probably by a reduction in the free volume. From the calculated data, it can be seen that the rate of

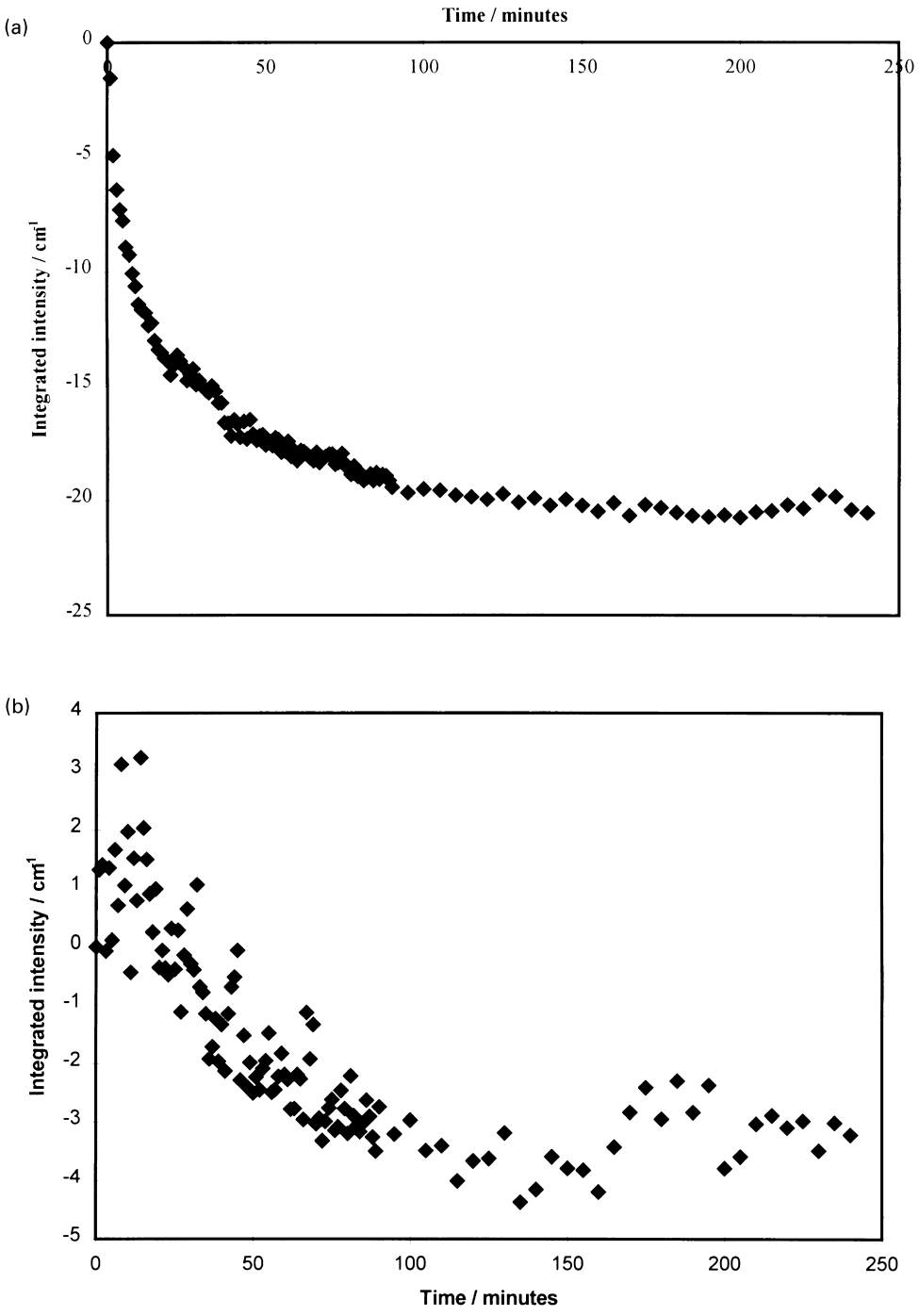

Fig. 11. Comparison of the integrated intensity changes of ν(C = O) band in the presence of methanol for: (a) 5.0% crystallinity; (b) 27.0% crystallinity.

methanol sorption into PET is faster than the rate of water sorption, most probably due to the accompanying swelling processes. We have seen evidence of a high wavenumber feature in the ν(OH) spectral region which could be interpreted as either 'free' methanol or methanol hydrogen bonded to PET. A similar effect was reported by Fieldson and Barbari during the sorption of methanol into PAN [10].

References

[1] Veith WR. Diffusion in and through polymers: principles and application. New York: Oxford University Press, 1991.
[2] Mark JE, editor. Physical properties of polymers handbook. New York: American Institute of Physics, 1996.
[3] Hornandez RJ, Giani JR, Baner AL. Proc. Techn. Association of the Pulp and Paper Industry (TAPPI). 1984 Conference, p. 107–31 and references therein.

[4] Baker RW, Cussler EL, Eykamp W, Koros WJ, Riley RL, Strathmann H. Membrane separation systems: recent development and future directions. Park Ridge, NJ: Noyes Data Corp, 1991.
[5] Grassie N, Scott G. Polymer degradation and stabilisation. Cambridge: Cambridge University Press, 1985.
[6] Costley CT, Dean JR, Newton I, Carroll J. Anal Comm 1997;34(3):89.
[7] Comyn J. Polymer permeability. New York: Elsevier, 1985.
[8] Vergnaud JM. Liquid transport properties in polymeric materials. Englewood Cliffs, NJ: Prentice Hall, 1991.
[9] Crank J, editor. The mathematics of diffusion 2. Oxford: Clarendon Press, 1994.
[10] Fieldson GT, Barbari TA. Polymer 1993;34:1146.
[11] Fieldson GT, Barbari TA. AIChE J. 1995;41:795.
[12] Windle AH, Comyn J, editors. Polymer permeability. London: Elsevier, 1986.
[13] Thomas NL, Windle AH. Polymer 1982;23:529.
[14] Berends AJ. J Appl Polym Sci 1989;37:901.
[15] Vieth WR, Howell JM, Hsieh JH. J Membrane Sci 1976;1:177.
[16] Pereira MR, Yarwood J. J Chem Soc Faraday Trans 1996;92:2737.
[17] Langevin D, Grenet J, Saiter JM. Eur Polym J 1994;30:30.
[18] Kloppers MJ, Bellucci F, Lantanision RM, Brennen JE. J Appl Polym Sci 1993;48:2197.
[19] Bellucci F, Nicodemo L. Corrosion 1993;49(3): 235.
[20] Rueda DR, Viksne A, Kajaks J, Balta-Cajella FJ, Zachmann HG. Macomol Symp 1995;94:259.
[21] Rueda DR, Varkalis A. J Polym Sci Part B: Polym Phys 1995;33:2263.
[22] Yasuda H, Stannett V. J Polym Sci 1962;57:907.
[23] Schühler, N, da Silva Sobrinho AS, Klemberg-Sapieha JE, Andrews M, Wertheimer MR. Society of Vacuum Coaters: 39th Annual Technical Conf. Proc. 1996, p. 285.
[24] Makarewics PJ, Wilkes GL. J Polym Sci Polym Phys Ed 1978;16:1559.
[25] Durning CJ, Russel WB. Polymer 1985;26:119.
[26] Durning CJ, Russel WB. Polymer 1985;26:131.
[27] Desai AB, Wilkes GL. J Polym Sci Symp 1974;46:291.
[28] Makarewics PJ, Wilkes GL. J Appl Polym Sci 1979;23:1619.
[29] Cottam L, Sheldon RP, Hemsley DA, Palmer RP. Polym Lett 1964;2:761.
[30] Beck HN. J Appl Polym Sci 1975;19:2601.
[31] Barson CA, Dong YM. Eur Polym J 1996;36(6):862.
[32] Popoola AV. J Appl Polym Sci 1993;49:2115.
[33] Richards PD, Weitz E, Ouderkirk AJ, Dunn DS. Macromolecules 1993;26:1254.
[34] Anderssen E, Zachmann HG. Colloid Polym Sci 1994;272(11):1352.
[35] Walls DJ. Appl Spec 1991;45(7):1193.
[36] Belali R, Vigoureux JM. Appl Spec 1994;48(4):465.
[37] Zajicek T. Thèse. 3ème cycle. Besaçon, 1987.
[38] Jabbari E, Pappas NA. J Mat Sci 1994;29:3960.
[39] Jabbari E, Pappas NA. Macromolecules 1995;28:6229.
[40] Barbari TA, Confort RM. J Polym Sci 1992;30B:1261.
[41] Schlotter NE, Furlan PY. Polymer 1992;33(16):3323.
[42] Hayes NW, Beamson G, Clark DT, Law DS-L, Raval R. Surface and Interface Analysis 1996;24(19):723.
[43] Walls DJ, Coburn JC. J Polym Sci Part B: Polym Phys 1992;30:887.
[44] van Alsten JG, Coburn JC. Macromolecules 1994;27:3752.
[45] Sammon C. Ph.D. thesis. Sheffield Hallam University, 1997.
[46] Lui C-PA, Neogi P. J Memb Sci 1988;35:207.
[47] Durning CJ, Rebenfeld L. J Appl Polym Sci 1984;29:3197.
[48] Durning CJ, Rebenfeld L, Russel WB, Weigmann WB. J Polym Sci Polym Phys Ed 1986;24:1321.
[49] Durning CJ, Rebenfeld L, Russel WB. Polym Engng Sci 1986;26:1066.
[50] Lui C-P, Lui A, Neogi P. J Macromol Sci Phys 1992;B31(3):265.
[51] Pereira MR, Yarwood J. J Chem Soc, Faraday Trans 1996;92(15): 2731.
[52] Pereira MR, Yarwood J. J Chem Soc, Faraday Trans 1996;92(15): 2737.
[53] Hajatdoost S, Yarwood J. J Chem Soc, Faraday Trans 1997; 93(8):1613.
[54] Cole KC, Guèvremont J, Ajji A, Dumoulin MM. Appl Spec 1994;48(12):1513.
[55] Hopfenberg HB. Permeability of plastic films and coatings to gases, vapours and liquids, 73. New York: Plenum Press, 1974 73.
[56] Kuipers NJM, Beenbackers AACM. Chem Engng Sci 1993; 48(16):2957.
[57] Sammon C, Yarwood J, Everall N. In preparation.